

OPEN

Trait-Based Comparison of Coral and Sponge Microbiomes

 Cara L. Fiore^{1,2,6*}, Jessica K. Jarett^{1,3,6}, Georg Steinert^{4,5} & Michael P. Lesser¹

Corals and sponges harbor diverse microbial communities that are integral to the functioning of the host. While the taxonomic diversity of their microbiomes has been well-established for corals and sponges, their functional roles are less well-understood. It is unclear if the similarities of symbiosis in an invertebrate host would result in functionally similar microbiomes, or if differences in host phylogeny and environmentally driven microhabitats within each host would shape functionally distinct communities. Here we addressed this question, using metatranscriptomic and 16S rRNA gene profiling techniques to compare the microbiomes of two host organisms from different phyla. Our results indicate functional similarity in carbon, nitrogen, and sulfur assimilation, and aerobic nitrogen cycling. Additionally, there were few statistical differences in pathway coverage or abundance between the two hosts. For example, we observed higher coverage of phosphonate and siderophore metabolic pathways in the star coral, *Montastraea cavernosa*, while there was higher coverage of chloroalkane metabolism in the giant barrel sponge, *Xestospongia muta*. Higher abundance of genes associated with carbon fixation pathways was also observed in *M. cavernosa*, while in *X. muta* there was higher abundance of fatty acid metabolic pathways. Metagenomic predictions based on 16S rRNA gene profiling analysis were similar, and there was high correlation between the metatranscriptome and metagenome predictions for both hosts. Our results highlight several metabolic pathways that exhibit functional similarity in these coral and sponge microbiomes despite the taxonomic differences between the two microbiomes, as well as potential specialization of some microbially based metabolism within each host.

Microbial symbionts have played a critical role in shaping the evolution of multicellular life by facilitating and promoting host defense¹, nutrient acquisition², and species diversification³. For example, in coral reef ecosystems, intracellular dinoflagellates in the Family Symbiodiniaceae occur as the primary mutualistic symbionts within the coral host and are essential to the survival and growth of the coral host, while receiving a suitable habitat and essential nutrients in return^{4,5}. Prokaryotic symbionts also contribute to the success of coral reef organisms, including corals and sponges^{6–9}, by providing bioactive compounds for chemical defenses^{10,11}, recycling host waste^{12,13}, and in some cases providing a reliable source of vitamins and nutrients^{14–17}. Numerous studies have characterized the taxonomic composition of microbes in corals and sponges^{18,19}; however, our understanding of the multiple functional roles of these symbionts is still incomplete.

Corals and sponges harbor remarkably diverse prokaryotic symbionts with thousands of unique taxa in many coral and sponge species^{20,21}. Many of these taxa persist across different host species (i.e., the core microbiome) over broad spatial scales^{9,22–24}, and in some cases these host-associated microbial communities are more stable over time than free-living communities^{24–26}, but see Sweet *et al.*²⁷ for another viewpoint. Recent work, however, has demonstrated a more pervasive environmental component to the microbiome composition of coral reef host organisms, with a high degree of overlap for environmental microbial taxa in sponges specifically²² although high specificity of prokaryotic taxa in sponges is also well documented^{19,22,28}. Sponges contain the highest number of unique taxa relative to other benthic host organisms, highlighting gaps in our knowledge in regards to microbiome structure and function within sponges and other coral reef organisms²². In both corals and sponges, the overall taxonomic composition of microbial consortia is influenced by host phylogeny^{19,27,28}, other symbionts (e.g.,

¹University of New Hampshire, Department of Molecular, Cellular and Biomedical Sciences, School of Marine Science and Ocean Engineering, Durham, NH, USA. ²Present address: Appalachian State University, Biology Department, Boone, NC, USA. ³Present address: AnimalBiome, Oakland, CA, USA. ⁴Institute for Chemistry and Biology of the Marine Environment, Carl-von-Ossietzky University Oldenburg, Wilhelmshaven, Germany. ⁵Present address: GEOMAR Helmholtz Centre for Ocean Research Kiel, Marine Symbioses, Kiel, Germany. ⁶These authors contributed equally: Cara L. Fiore and Jessica K. Jarett. *email: fiorec@appstate.edu

Symbiodiniaceae) and environmental factors^{19,27–31}, underscoring the multiple, complex influences on microbiome structure (reviewed for corals^{7,9,18}; sponges^{31,32}).

Recent metagenomic and metatranscriptomic studies on corals and sponges have revealed a complex picture of microbial functions. The cycling of essential nutrients, primarily carbon (C), nitrogen (N), sulfur (S), and phosphorus (P) (see below; reviewed in^{8,18,31,32}) has been the best studied to date. The fixation of carbon in the form of CO₂ by symbionts and subsequent translocation of photosynthate to the host is well documented for Symbiodiniaceae in corals but has also been observed for *Cyanobacteria* and Symbiodiniaceae in several sponges^{16,33,34}. The discovery of multiple carbon fixation pathways in coral- and sponge-associated microbes, including the Wood-Ljungdahl pathway, reverse tricarboxylic acid (TCA) cycle, and reductive acetyl-CoA pathway, indicate a far more complex system for carbon cycling and potential host-microbe interactions^{17,35–38} than previously believed. Furthermore, microbes in corals and sponges can transform N^{14,15}, S^{39,40}, P^{41,42}, and diverse organic compounds in dissolved organic matter^{43–47} into microbial biomass that can be consumed by the host or into compounds that provide direct or indirect benefits to the host (e.g., ammonia from fixed N₂). It is important to note, however, that microbial and host physiologies have not necessarily evolved towards beneficial interactions as a means of coexistence, even when translocation of metabolic products is considered^{14,16,17,48}. Arguably, it is more typical that each member is selected upon to survive in a complex system, often utilizing by-products of metabolism from other members (e.g., syntrophy) in an ecosystem that is the holobiont⁴⁹.

Different structural characteristics of corals and sponges create different microhabitats that influence the composition of their microbiomes. Both host organisms have an open system where microbes are exposed to environmental conditions in the surrounding seawater. Sponges contain multiple cell types that form different layers, as well as the aquiferous system, which includes choanocyte chambers for filtering water. Variability in the flow rate of water through the sponge body creates microhabitats based on oxygen gradients¹², facilitating physiologically diverse microbial communities. Scleractinian corals contain an outer mucus layer, and tissue layers with and without algal symbionts, as well as a calcium carbonate skeleton, each of which forms a unique microhabitat^{7,50,51}. Corals also exhibit a strong diurnal oxygen gradient, with hyperoxia during the day from algal photosynthesis, and hypoxia at night⁵², creating temporally-mediated niches for diverse microbial metabolic processes, such as nitrogen fixation^{8,14}. The different characteristics of each host species and their co-occurrence in the same habitat provide an opportunity to examine both specialized and convergent aspects of their microbiomes. Similar comparisons have been made within phylogenetically diverse sponge microbiomes, which indicated functional convergence in five main areas: (a) nitrogen metabolism, (b) nutrient utilization and nutritional interactions with the host, (c) resistance to environmental and host-specific stress, (d) eukaryotic-like proteins involved in host-microbe interaction, and (e) horizontal gene transfer⁵³. However, there are few studies that have compared functional diversity and potential convergence in microbiomes between invertebrate phyla^{22,54}.

Here, we integrate previously published^{17,55} RNAseq data from the microbiome of the great star coral, *Montastraea cavernosa*, and the giant barrel sponge, *Xestospongia muta*, along with new analyses of these metatranscriptomes, to advance our understanding of microbiome function in these two abundant and phylogenetically distant host species in the Caribbean basin. The analysis presented here includes a unique approach that directly analyzes quality-trimmed short-reads from RNA sequencing. This short-read analysis is paired with an assembly of each metatranscriptome to allow for more in-depth analysis of metabolic pathways (Fig. 1). While advances in computation now make *de novo* metatranscriptome assembly a more feasible approach than it used to be, the complementary approaches provide novel insight into the functional repertoire of two distinct host species. Furthermore, while there is a strong interest in environmental microbiome analysis^{22,56}, there are no published studies (to our knowledge) that compare metatranscriptome profiles across host phyla. The scleractinian coral, *M. cavernosa* exists in two co-occurring morphs, orange and brown; the orange morph contains more abundant cyanobacteria and is capable of much higher rates of nitrogen fixation than the brown morph^{14,55}. *Xestospongia muta* is an abundant sponge that can grow to massive sizes on many Caribbean reefs, with important implications for nutrient dynamics in those habitats^{57–59}. Finally, we compared prokaryotic community predictions from 16S rRNA gene amplicon sequences^{55,60} to functional activity to assess the accuracy of predictive approaches (Fig. 1). While this study is limited to the analysis of one coral species and one sponge species, the comparison of the two hosts sheds light on core processes related to symbiosis.

Results and Discussion

Comparison of total and active microbial communities. The total microbial community, as measured by 16S rRNA amplicon sequencing in previous work^{55,60} differs between *M. cavernosa* and *X. muta* hosts (Supplementary Fig. S1). Data from the current study shows that the target host species also differed in their active communities under the environmental conditions when collections occurred, determined here by mapping mRNA reads to a reference database to assign taxonomy (Fig. 2, Supplementary Information S1, Supplementary Information S2). Notably, in *M. cavernosa* and *X. muta*, *Cyanobacteria*, *Proteobacteria*, and *Firmicutes* were more transcriptionally active than would be predicted by the abundance of 16S rRNA genes (Supplementary Fig. S1; Supplementary Information S2). These major groups may underlie functional characteristics in the host microbiomes described below. Meanwhile, the largest proportion of the active community in *M. cavernosa* included *Beta*- and *Gammaproteobacteria* and *Bacteroidetes* and in *X. muta* included *Cyanobacteria*, *Beta*- and *Alphaproteobacteria*. The differences highlighted between the total and active groups within each host and between host communities and may drive some of the difference visualized by principal components analysis (PCA) (Fig. 2).

The taxonomic differences highlighted here between the *M. cavernosa* and *X. muta* microbiomes used in this study could imply functional differences in activity and potentially differences in niche partitioning within the holobiont^{61,62}. Alternatively, similar functional traits may dominate metabolic activity in the two different host taxa, as has been described in other studies^{53,63–65}. We address this question below by comparing the functional

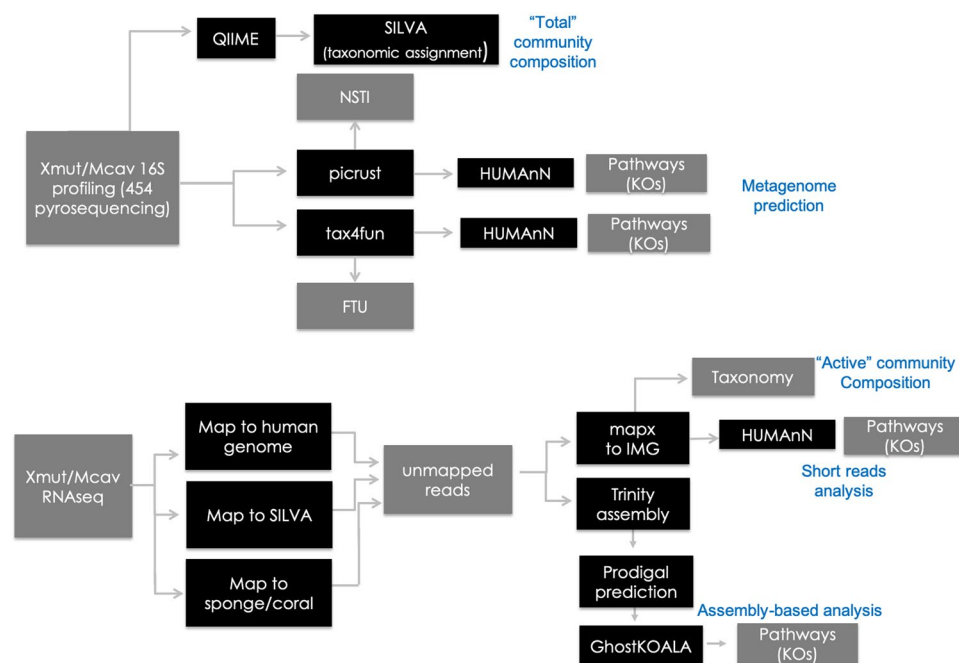


Figure 1. Overview of metatranscriptome and microbiome profiling methods. Gray boxes represent data types while black boxes represent a data analysis program and/or process.

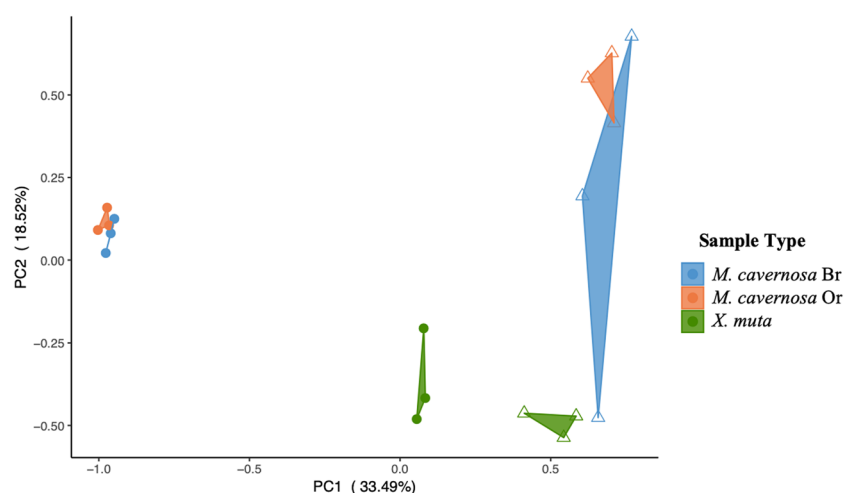


Figure 2. Principal components analysis of active and total microbial communities in the coral *Montastraea cavernosa* (brown (Br) and orange (Or) color morphs) and sponge, *Xestospongia muta*. Open triangles represent total microbial communities (16S rRNA genes) and closed circles represent active communities (mRNA). Total microbial communities were identified by 16S rRNA gene profiling performed previously (Fiore *et al.*⁶⁰; Jarett *et al.*⁵⁵). Active microbial communities were identified by querying prokaryotic genomes in the Integrated Microbial Genomes (IMG) database (see Methods).

profile of *M. cavernosa* and *X. muta* using metatranscriptomics. We note however, that samples of coral and sponge were collected at the same depth (15 m) but at different times of day (morning and midday, respectively) and in different locations in the Caribbean. These temporal and environmental factors could influence differences in both the composition of the active community profile (identity) and the functional profile (transcripts) between the two host organisms.

Functional overview of the sponge and coral microbiome. Profiles of functional gene expression were generated with two approaches; the first provided a functional profile of metabolic pathways (short-read analysis) and the second provided more in-depth analysis of specific metabolic pathways (assembly analysis) (Fig. 1). The short-read analysis used the mapx algorithm to map RNA reads to the IMG prokaryotic genomes followed by analysis with HUMANn⁶⁶ to produce estimates of coverage and abundance for KEGG⁶⁷ pathways

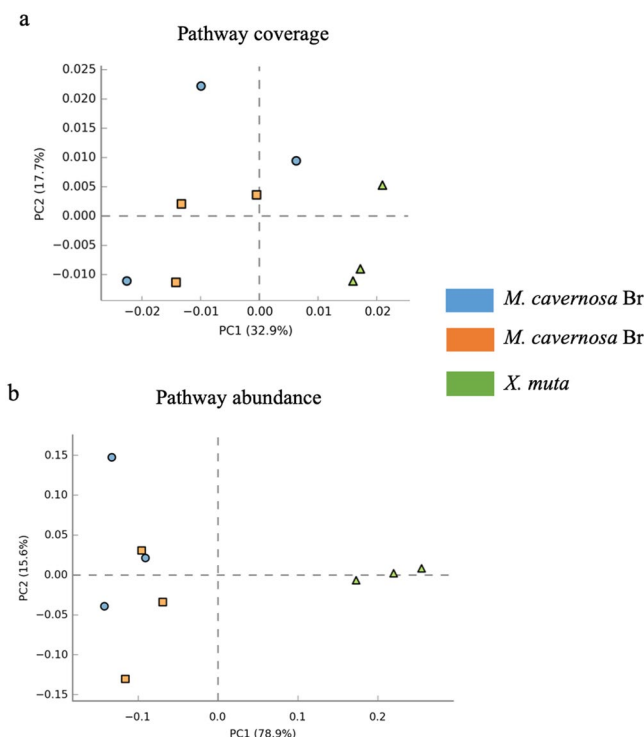


Figure 3. Principal components analysis (PCA) of KEGG Orthology pathways⁶⁷ based on coverage (a) and relative abundance (b) in the coral, *Montastraea cavernosa* (brown (Br) and orange (Or) color morphs) and sponge, *Xestospongia muta*. KEGG Orthology pathways were assigned, and relative abundance and coverage were calculated, with HUMAnN⁶⁶ based on putative mRNA reads from the prokaryotic community.

(see Methods). These results were subsequently analyzed in STAMP⁶⁸ by PCA and analysis of variance (ANOVA) with an effect size threshold of 0.8 and Benjamin-Hochberg FDR correction for p -values⁶⁹ (see Supplementary Information S1). Meanwhile, assembly of the RNA reads into putative mRNA transcripts (i.e., contigs) allowed us to map and visualize gene expression for specific KEGG pathways of interest. Hereafter, we refer to read coverage or abundance (from the short-read analysis) and transcript presence (assembly analysis) in a metabolic pathway. Reads per sample varied across samples but were not significantly different between coral, *M. cavernosa* (average 40,832,418 ($\pm 3,815,419$)⁵⁵), and sponge, *X. muta* (42,230,246 ($\pm 9,246,767$)¹⁷) (t -test, $p = 0.01$). We note, however, that differences in time of sampling limit the interpretation of our comparisons to some extent.

In the short-read analysis, we compared the relative coverage and abundance of KOs from symbiont reads in the color morphs of *M. cavernosa* and *X. muta*. There were no differences in pathway abundances between coral color morphs (ANOVA, $p > 0.05$, Fig. S2), so corals were pooled for further analyses. The lack of significant differences within the corals was initially surprising because expression differences were observed in earlier analysis of this dataset⁵⁵; however, the analysis here is based on annotation of short-reads which may highlight an important methodological consideration for future work. The previous work⁵⁵ used assembly analysis and observed some, but few overall, differentially expressed genes between the color morphs. The assembly approach may be more sensitive to differences in transcript abundance. Furthermore, previous work indicated no significant difference in microbial community composition between the color morphs of *M. cavernosa*⁵⁵. When considering all pathways, coral and sponge samples could be separated along by PCA (Fig. 3a), particularly by pathway abundance (Fig. 3b). However, *M. cavernosa* color morphs were always intermingled (Supplementary Fig. S2). These data suggest that the metabolic differences between host species are much larger than those between coral morphs. This difference between species may be largely driven by differences in transcript abundance or differences in the types of pathways they express; each is described below.

Pairwise analysis in STAMP of pathway coverage between *M. cavernosa* and *X. muta*, revealed six pathways that were significantly different in coverage between the pooled *M. cavernosa* and *X. muta* samples (ANOVA, adjusted $p = 0.003$ – 0.047 , Table 1) (Fig. 4), with an additional five pathways below the effect size threshold of 0.8 (Supplementary Fig. S3). Linoleic acid metabolism, phosphonate and phosphinate metabolism, other glycan degradation, and biosynthesis of siderophore group nonribosomal peptide pathways had significantly higher coverage in *M. cavernosa*, while chloroalkane and chloroalkene degradation and proteasome pathways were significantly higher in coverage in *X. muta* (Fig. 4).

None of the differentially covered pathways were also significantly different in terms of abundance between *M. cavernosa* and *X. muta* (Fig. 5). Six other pathways were significantly different in abundance between *M. cavernosa* and *X. muta* (Table 1, ANOVA, adjusted $p = 0.008$ – 0.04), with an additional 31 pathways below effect size threshold of 0.8, including lipid metabolism and vitamin B metabolism which have been described as important symbiont pathways in sponges previously (Supplementary Fig. S4). Some metabolic pathways below the effect

Pathway	p-values	p-values (corrected)	Mcav: mean rel. freq. (%)	Mcav: std. dev. (%)	Xmuta: mean rel. freq. (%)	Xmuta: std. dev. (%)	Difference between means	95.0% lower CI	95.0% upper CI
Pathway Coverage									
Biosynthesis of siderophore group nonribosomal peptides	0.005	0.040	0.290	0.097	0.083	0.001	0.207	0.096	0.319
Chloroalkane and chloroalkene degradation	<0.001	0.009	0.132	0.295	1.085	0.115	−0.953	−1.32	−0.587
Linoleic acid metabolism	<0.001	0.008	0.837	0.153	0.000	0.000	0.837	0.661	1.01
Other glycan degradation	0.001	0.018	0.525	0.146	0.054	0.077	0.471	0.267	0.674
Phosphonate and phosphinate metabolism	<0.001	0.010	0.440	0.123	0.033	0.046	0.408	0.257	0.559
Proteasome	0.001	0.019	0.083	0.049	0.221	0.004	−0.138	−0.194	−0.082
Pathway Abundance									
Cell cycle - Caulobacter	0.011	0.047	0.43	0.10	2.26	0.31	−1.83	−2.72	−0.94
Fatty acid biosynthesis	<0.001	0.004	0.76	0.10	1.73	0.09	−0.98	−1.18	−0.77
Lipoic acid metabolism	0.003	0.021	0.22	0.13	1.24	0.16	−1.02	−1.41	−0.63
Oxidative phosphorylation	0.001	0.011	21.13	6.15	3.06	1.06	18.07	11.01	25.14
Photosynthesis	<0.001	0.003	25.60	4.94	1.93	1.91	23.66	17.54	29.78
RNA polymerase	0.003	0.019	0.16	0.06	1.41	0.13	−1.24	−1.60	−0.89

Table 1. Summary of pair-wise comparisons of pathway coverage and abundance between the coral, *Montastraea cavernosa* (Mcav) and the sponge, *Xestospongia muta* (Xmuta). The functional profiles were derived from short-read analysis using IMG prokaryotic genomes and processed with the program HUMAnN⁶⁶ to assign pathway coverage and abundance. Analysis of variance and pair-wise comparisons were performed in the program STAMP⁶⁸ with an effect size threshold 0.8 and Benjamin -Hochberg correction for multiple comparisons.

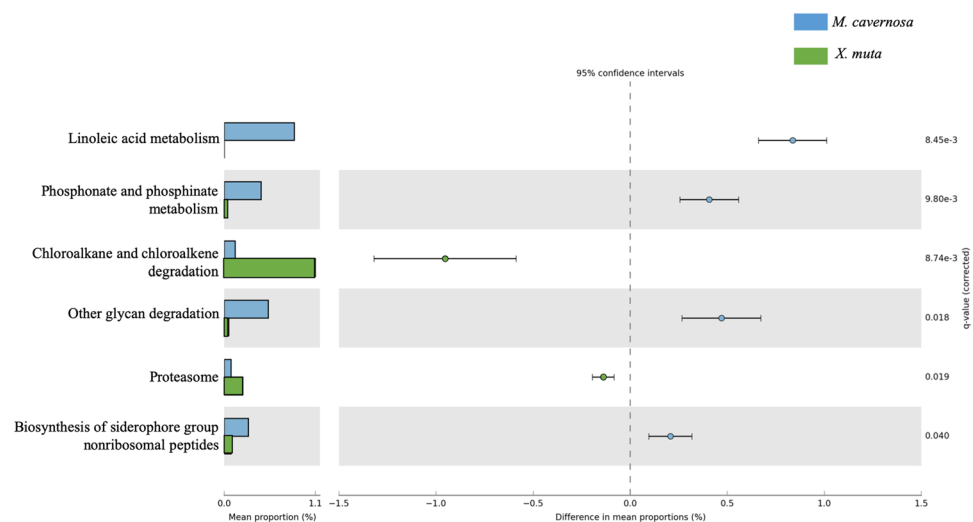


Figure 4. Pair-wise comparisons between KEGG Orthology pathway⁶⁷ coverage in the coral, *Montastraea cavernosa* (n = 6) and sponge, *Xestospongia muta* (n = 3). Difference between groups was assessed with a Welch's *t*-test with Benjamin-Hochberg FDR correction for q-values and a relative effect size of 0.8. KEGG Orthology pathways were assigned, and relative abundance was calculated, with HUMAnN⁶⁶ based on putative mRNA reads from the prokaryotic community.

size threshold for pathway abundance or coverage did overlap between the two host species, such as chloroalkane metabolism (Supplementary Fig. S4). The limited overlap in pathways between the two host organisms that were statistically significant in coverage or abundance, points to a mix of both gene content and gene expression that differ between the *M. cavernosa* and *X. muta* microbiomes.

Lastly, we leveraged the previously published 16S rRNA gene profiling in metagenome prediction to compare the predicted functional profile with the metatranscriptome functional profile. In our study, the HUMAnN-produced KEGG Orthology (KOs) from PICRUSt and Tax4Fun were compared with HUMAnN-produced KOs from metatranscriptome (see Methods). The NSTI values associated with PICRUSt predictions and the FTU values associated with the Tax4Fun predictions were relatively high (Supplementary

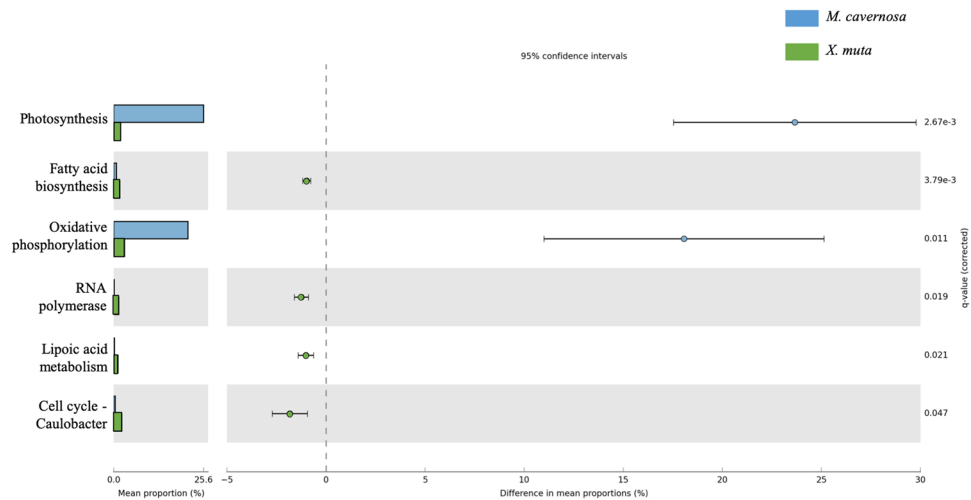


Figure 5. Pair-wise comparisons between KEGG Orthology pathway⁶⁷ abundance in the coral, *Montastrea cavernosa* (n = 6) and sponge, *Xestospongia muta* (n = 3). Difference between groups was assessed with a Welch’s *t*-test with Benjamin-Hochberg FDR correction for q-values and a relative effect size of 0.8. KEGG Orthology pathways were assigned, and relative abundance was calculated, with HUMAnN⁶⁶ based on putative mRNA reads from the prokaryotic community.

Prediction	correlation	<i>t</i>	<i>p</i> -value
Coverage			
Tax4Fun-HUMAnN			
Xmut	0.82	16.5	<0.001
Mcav	0.74	12.9	<0.001
PICRUSt-HUMAnN			
Xmut	0.82	16.5	<0.001
Mcav	0.78	14.3	<0.001
Abundance			
Tax4Fun-HUMAnN			
Xmut	0.36	4.6	<0.001
Mcav	0.06	0.74	0.46
PICRUSt-HUMAnN			
Xmut	0.49	6.7	<0.001
Mcav	0.09	1.04	0.3

Table 2. Summary of Pearson’s product-moment correlations between predicted KEGG Orthology⁶⁷ pathway coverage or abundance and sequenced metatranscriptomes in the sponge and coral samples. KEGG Orthology pathways were assigned, and pathway coverage and abundance were calculated, with HUMAnN⁶⁶ based on mRNA reads or with HUMAnN following PICRUSt¹¹⁹ or Tax4Fun¹²⁰ based on 16S rRNA gene profiling. Significant ($\alpha = 0.05$) *p*-values are in bold.

Table S1). The values of NSTI and FTU provide an estimate of accuracy of the functional prediction based on the taxonomic similarity between the query and reference taxa (see Methods). Here, the high values indicate low similarity between the reference taxa and our samples, and less reliable predictions. Despite the high NSTI and FTU values, there was strong correlation between the functional profiles of the metatranscriptome and metagenome predictions for both coverage and abundance (Table 2). Moreover, there was overlap in the top 25 abundant pathways based on short read analysis of the metatranscriptome and the top 25 pathways predicted based on 16S rRNA gene profiling (Table 3; Supplementary Table S2). Ultimately, the use of multiple approaches (short read analysis, assembly analysis, and metagenome prediction) to compare the functional profiles of *M. cavernosa* and *X. muta* uncovered two key results: (1) similar to other studies, the overlap in functional profiles between the metatranscriptome and the metagenome predictions was relatively high (Table 2), providing support for these metagenome prediction programs in future work, and (2) we observed indications of both convergence and specialization within the host microbiomes.

Functional equivalence in sponge and coral microbiomes. Reads and transcripts were identified for multiple pathways involved in elemental cycles, including carbon (C), nitrogen (N), and sulfur (S), in both host species. Previous studies have also highlighted the importance of major C and N pathways in sponge- and

Pathway	Sponge (<i>X. muta</i>)	Coral (<i>M. cavernosa</i>)	Unique to <i>M. cavernosa</i>
ko00195: Photosynthesis	0.019	0.255	ko00830: Retinol metabolism
ko00190: Oxidative phosphorylation	0.030	0.211	ko05200: Pathways in cancer
ko00970: Aminoacyl-tRNA biosynthesis	0.015	0.049	
ko00450: Selenocompound metabolism	0.015	0.026	
ko00010: Glycolysis / Gluconeogenesis	0.015	0.023	
ko00750: Vitamin B6 metabolism	0.020	0.018	
ko00630: Glyoxylate and dicarboxylate metabolism	0.013	0.018	
ko00620: Pyruvate metabolism	0.013	0.018	
ko00020: Citrate cycle (TCA cycle)	0.020	0.014	
ko00710: Carbon fixation in photosynthetic organisms	0.001	0.013	
ko00270: Cysteine and methionine metabolism	0.011	0.013	
ko00720: Carbon fixation pathways in prokaryotes	0.015	0.011	
ko00290: Valine, leucine and isoleucine biosynthesis	0.031	0.011	
ko00660: C5-Branched dibasic acid metabolism	0.029	0.011	
ko00030: Pentose phosphate pathway	0.014	0.011	
ko03010: Ribosome	0.111	0.010	
ko00250: Alanine, aspartate and glutamate metabolism	0.013	0.008	
ko00061: Fatty acid biosynthesis	0.017	0.008	
ko00260: Glycine, serine and threonine metabolism	0.012	0.007	
ko03018: RNA degradation	0.041	0.007	
ko00770: Pantothenate and CoA biosynthesis	0.017	0.007	
ko00670: One carbon pool by folate	0.012	0.007	
ko00480: Glutathione metabolism	0.007	0.007	
ko03060: Protein export	0.021	0.006	
ko00910: Nitrogen metabolism	0.005	0.006	
Pathway	Sponge (<i>X. muta</i>)	Coral (<i>M. cavernosa</i>)	Unique to <i>X. muta</i>
ko03010: Ribosome	0.111	0.010	ko05110: Vibrio cholerae infection
ko03018: RNA degradation	0.041	0.007	ko00563: Glycosylphosphatidylinositol(GPI)-anchor biosynthesis
ko00290: Valine, leucine and isoleucine biosynthesis	0.031	0.011	ko00642: Ethylbenzene degradation
ko00190: Oxidative phosphorylation	0.030	0.211	ko00909: Sesquiterpenoid biosynthesis
ko00660: C5-Branched dibasic acid metabolism	0.029	0.011	ko00621: Dioxin degradation
ko04112: Cell cycle - Caulobacter	0.022	0.004	ko05143: African trypanosomiasis
ko03060: Protein export	0.021	0.006	
ko00750: Vitamin B6 metabolism	0.020	0.018	
ko00020: Citrate cycle (TCA cycle)	0.020	0.014	
ko00195: Photosynthesis	0.019	0.255	
ko00061: Fatty acid biosynthesis	0.017	0.008	
ko00770: Pantothenate and CoA biosynthesis	0.017	0.007	
ko00450: Selenocompound metabolism	0.015	0.026	
ko04122: Sulfur relay system	0.015	0.004	
ko00720: Carbon fixation pathways in prokaryotes	0.015	0.011	
ko00010: Glycolysis / Gluconeogenesis	0.015	0.023	
ko00970: Aminoacyl-tRNA biosynthesis	0.015	0.049	
ko00030: Pentose phosphate pathway	0.014	0.011	
ko03020: RNA polymerase	0.014	0.002	
ko00730: Thiamine metabolism	0.014	0.004	
ko00630: Glyoxylate and dicarboxylate metabolism	0.013	0.018	
ko00620: Pyruvate metabolism	0.013	0.018	
ko00250: Alanine, aspartate and glutamate	0.013	0.008	
ko00260: Glycine, serine and threonine metabolism	0.012	0.007	
ko00785: Lipoic acid metabolism	0.012	0.002	

Table 3. Top 25 metabolic pathways of coral and sponge (continued) microbiomes based on short-read analysis. The relative abundance of the pathway is shown for each pathway and host. Pathways also in the top 25 pathways predicted by PICRUST¹²⁶ and Tax4Fun¹²⁷ are bolded.

coral-microbe symbioses^{18,53,70,71}. In the current study, there was often overlap in the presence of major pathways for nutrient acquisition and/or catabolism, with only a few specific pathways (i.e., DNRA, sulfur oxidation) exclusive to sponges or corals. We highlight here the complexity in comparing nutrient pathways at both a broad (e.g., “N cycling”) and fine-scale level (e.g., “ammonia oxidation pathway”), which makes generalizations more difficult, but the latter provides more biologically meaningful information. In terms of C fixation and catabolism, photosynthesis and oxidative phosphorylation were evident in both host species but were approximately 24% and 18% more abundant in corals, respectively (Fig. 5). Because of the differences detected in C metabolism in both the short-read analysis and assembly analysis we discuss this topic further in the “Specialization” section below.

In contrast to central C metabolism, no pathways were identified as significantly different between host taxa for N metabolism based on the short-read analysis, potentially indicating high convergence in N cycling between host species similar to previous studies on sponges⁵³. However, we note that the assembly analysis revealed some differences in presence of transcripts (Fig. 6). In both host species complete nitrification, which converts ammonia to nitrate, was not detected. Nitrification has been documented in corals previously^{72,73} and transcripts for the first step of ammonia oxidation were observed only for the *M. cavernosa* (Fig. 6). The lack of nitrification transcripts for *X. muta* was surprising as nitrification is known to occur in this sponge^{57,59}. It may be that nitrification was not occurring at the time of sampling. In support of this, *Nitrospirae* bacteria known to contribute to nitrification were documented in the total community but were a minor portion of the active community (Supplementary Information S2). This result is supported by published studies documenting high variability in pumping activity in *X. muta*⁵⁸ and suggests corresponding variability in nitrification activity, an area for further work.

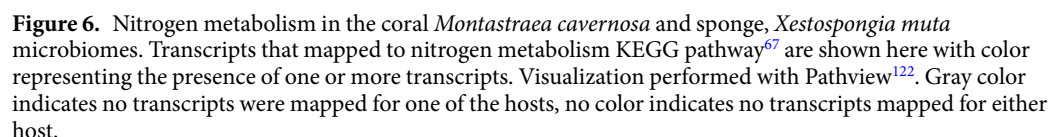
Denitrification was also not detected in either host species. Dentrifying bacteria have been observed in coral^{72,74} and recently, denitrification rates were documented for three coral species in the Red Sea⁷¹. Thus, either denitrification does not occur in this coral, *M. cavernosa*, or it was not occurring at the time of sampling. In contrast, the sponge microbiome contained several, but not all steps of the denitrification pathway and genes involved in dissimilatory nitrate reduction to ammonia (DNRA), indicating the existence of anaerobic dissimilatory nitrogen processes in this host. There may be more opportunity for anaerobic microhabitats within the sponge host, due to variable pumping activity, than within the coral. However, sampling for this study was conducted in the mid-morning for *X. muta* and midday for *M. cavernosa* and it is possible that this is a factor in the differences detected here between host organisms. Furthermore, it is likely that some anaerobic metabolism could occur in the coral microbiome at night due to diurnal fluctuations in tissue pO_2 . However, spatial separation can also allow for simultaneous aerobic and anaerobic processes and pO_2 was not found to influence denitrification and nitrogen fixation rates in Red Sea stony coral⁷¹. Dissimilatory metabolism thus appears to represent a mix of potential convergence (e.g., lack of significant differences based on short-read analysis) and some specialization (i.e., DNRA in *X. muta*) between host species.

Assimilation of N using glutamate dehydrogenase (*gdhA*), which is generally used during times of nitrogen excess⁷⁵, was evident in both host species indicating a common form of N assimilation (Fig. 6). However, in *M. cavernosa*, transcripts were also recovered for the canonical glutamine synthetase and glutamate synthase (GS-GOGAT) pathway, indicating that at least at the time of sampling these microbes were not nitrogen limited. Interestingly, transcripts representing *nifH*, a component of the nitrogenase enzyme for nitrogen fixation were recovered only from *M. cavernosa*, highlighting the potential for ammonia concentration gradients within the coral host. These results support a critical role of nitrogen recycling with the holobiont.

In terms of S cycling, there was overlap in coverage of S related pathways in the two host species, although some pathways were more complete in *X. muta* than *M. cavernosa*. No transcripts corresponding to dimethylsulfoniopropionate (DMSP) production were observed in *M. cavernosa*, which was expected as this pathway is thought to be driven by Symbiodiniaceae⁴¹ and those eukaryotic transcripts were not included in this analysis. While both hosts expressed sulfate assimilation genes, only *M. cavernosa* expressed sulfate transport and only *X. muta* expressed sulfur oxidation genes and other sulfur metabolism genes such as alkanesulfonate monooxygenase (*ssuD*, Fig. 7). For example, sulfur assimilation by sulfate reduction to adenylyl sulfate (APS), 3'-phosphoadenylyl sulfate (PAPS), and to sulfide, was observed in each host microbiome. However, other steps in organic sulfur compound metabolism differed between the hosts, potentially indicating that these microbial communities utilize or have available to them different compounds depending on their host. Furthermore, the assimilation of sulfonates in *X. muta* microbiome could indicate sulfur-limiting conditions⁷⁶.

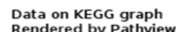
Evidence of sulfur oxidation in microbiomes of other sponges^{77,78}, corals⁷⁹, and other invertebrates⁸⁰ suggests this is a common energy source for symbiotic microbes, although it could be regulated by diurnal fluctuations in oxygen concentration in *M. cavernosa*. Transcripts for a thiosulfate transporter (*cysP*) were recovered from *M. cavernosa* (Fig. 7), which could represent an important source and means of obtaining sulfur for coral symbionts. Symbiotic bacteria in other systems also show elevated expression of genes related to sulfur uptake and metabolism in the symbiotic state relative to the free-living state⁷⁶; this may represent an important trait in symbiotic bacteria.

Pathway predictions (Tax4Fun and PICRUSt) highlighted several other major pathways with overlap between host species although there were some differences in pathway abundance. This high overlap occurs despite deep phylogenetic differences in the host taxa and differences in sampling location and time. The similar pathways include vitamin metabolism ketone body metabolism, phosphonate and phosphinate metabolism, and siderophore production. Vitamin metabolism has been highlighted as an important trait for sponge-microbe symbioses^{53,70} and may be critical for stability of symbiosis under environmental stress such as ocean acidification⁷⁰. Our results indicate that despite differences in host taxa, vitamin metabolism remains an abundant and likely important metabolic pathway for symbiont microbiomes. Transcripts for ketone body metabolism were present in both microbiomes but were more abundant in the coral microbiome (Table 3, Supplementary Fig. S6). Diverse bacteria can produce and degrade ketone molecules either anaerobically⁸¹ or aerobically⁸². In addition to their role in central metabolism, ketones have been of interest for years as bioactive compounds from soft corals



Montastraea cavernosa and *X. muta* both contained prokaryotic pathways of phosphonate and phosphate metabolism (Fig. 4). Pathway coverage was higher in *M. cavernosa*, which is intriguing as corals and dinoflagellates (i.e., Symbiodiniaceae symbionts of corals) use phosphonates, which contain a phosphorus-carbon bond, in lipid metabolism to form phosphonolipids in cell membranes^{86–88}. Phosphonate compounds are an abundant component of the dissolved organic phosphorus pool in marine systems^{89–91}, but inorganic phosphorus is typically very low in concentration in coral reef seawater^{92,93}. Thus, host-derived phosphonate compounds may be an important source of phosphorus for the coral microbiome community. Indeed, at least 13 coral species produce phosphonate and their associated microbes possess genes for phosphonate degradation⁴². Here, we add to these data by demonstrating not just presence but expression of phosphonate metabolizing genes in the coral holobiont. Furthermore, to our knowledge, there is limited information available on the presence and activity of phosphonate compounds and metabolism in invertebrates^{87,93} (and references therein). However, phosphonate metabolism is prevalent in marine microbes⁹¹ and our results here as well as another recent report of phosphonate metabolism in sponges⁹⁴, indicate at least some metabolic activity of phosphonate compounds by sponge microbes.

Specialization within the sponge and coral microbiomes. The short-read analysis of *X. muta* and *M. cavernosa* metatranscriptomes and the metabolic pathway predictions based on 16S rRNA gene profiling of the coral and sponge^{55,60} predicted higher abundance of xenobiotic metabolism (e.g., atrazine, nitrotoluene degradation) in sponges than in corals (Table 3, see Supplementary Information S1 for further discussion of metagenome prediction). The term ‘xenobiotic’ is used in KEGG ontology and refers to compounds not made by the organism itself, although in our dataset it is possible that some of these compounds are produced by the host or associated microbial community. In the short-read analysis, this difference between host species was supported by both pathway coverage and abundance (i.e., chloroalkane degradation, Fig. 4, Supplementary Fig. S4). Furthermore, the unique metabolic pathways observed in *X. muta* based on short-read analysis included several xenobiotic metabolic pathways (Table 3). Thus, multiple lines of evidence highlight the biosynthetic and



We suggest that photosynthesis, to some extent, is a specialized trait within the coral microbiome. While the presence of photosynthesis and C-fixation pathways were expected as both host species harbor photoautotrophic symbionts. The elevated abundance of reads that mapped to the photosynthesis pathway (Fig. 5) in coral prokaryotic microbiomes was surprising, as this process is generally attributed to the Symbiodiniaceae in corals. Further, the density of microbes is likely to be lower in *M. cavernosa* than in *X. muta*, a high microbial abundance sponge¹¹¹, underscoring the significance of our results. *Cyanobacteria* and other phototrophic bacteria (e.g., certain clades of *Proteobacteria* and *Chloroflexi*) within coral tissues^{28,112} or trapped in mucus^{113–115}, as well as recently described symbiotic apicomplexan protists¹¹⁶ may have contributed to elevated abundance of genes associated with photosynthetic pathways in the *M. cavernosa* microbiome samples and could be an important energy source for the microbiome in healthy corals. Some sponges harbor Symbiodiniaceae as symbionts, however, *X. muta* is not known to contain this dinoflagellate as a symbiont and the transcripts identified here likely come from *Cyanobacteria*, which constitute a major proportion of the microbial community in *X. muta*^{60,117,118}. Similarly, transcripts for carbon fixation in photosynthetic organisms were also more abundant in the coral than sponge microbiome (Supplementary Fig. S5), supporting the significantly higher abundance of this pathway in coral in the short-read analysis.

SCIENTIFIC REPORTS | (2020) 10:2340 | <https://doi.org/10.1038/s41598-020-59320-9>

could reflect high heterotrophic metabolism in microbes utilizing coral mucus, a phenomenon described previously^{115,116}. However, the difference abundance of oxidative phosphorylation pathways between *M. cavernosa* and *X. muta* is somewhat surprising as heterotrophic metabolism is also expected in *X. muta* based on the microbial community composition^{115,119} and this pathway was highlighted previously as abundant in sponge microbial communities⁷⁰. Further genomic work is needed to elucidate if, and what are the biological relevance of such differences between the *M. cavernosa* and *X. muta* communities.

Conclusions

Our data support the evolutionary convergence in the microbiome functions of the coral *Montastraea cavernosa* and the sponge, *Xestospongia muta*, highlighted here by the few significant differences in functional gene profile based on short-read analysis. Despite the presence of Symbiodiniaceae in *M. cavernosa* and absence in *X. muta*, there is significant overlap in many KEGG prokaryotic cellular and metabolic pathways. In particular, similarities in N (e.g., nitrification and nitrogen assimilation via glutamate dehydrogenase), P (e.g. phosphonate metabolism), and S (e.g., sulfate reduction) cycling were observed based on short-read analysis of mRNA. A similar observation has also been made across sponge taxa^{62,120–122} and in other microbiome systems^{64,123–125}, supporting the notion that conservation of function rather than taxonomy is a common characteristic of symbiont communities. To our knowledge, however, functional convergence has not been specifically investigated within coral hosts. Further, we also observed differences in symbiont diversity and pathway coverage that may underlie specialized functional characteristics of each microbiome reflective of distinct host-microbe interactions. Surprisingly, photosynthesis and C-fixation were more abundant in *M. cavernosa* which also hosts Symbiodiniaceae while secondary metabolite metabolism, and potentially related pathways (e.g., fatty acid metabolism) appeared to be of more significance in *X. muta*. We propose several additional questions for further research that our results have highlighted. One is that there are no metatranscriptome studies that have examined diurnal differences in the coral microbiome, but such work could shed light on oxygen-dependent microbial activity. Similarly, while denitrification was not detected in *M. cavernosa*, it would be worth investigating this process further as this coral species hosts N-fixing bacteria and the two N processes were recently shown to be linked in coral⁷⁰. Separately, phosphorus cycling is of recent interest in holobiont metabolism^{122,126,127}, and specifically, the role of Symbiodiniaceae in the production of phosphonates and whether this source of phosphorus is available to microbes associated with sponges (with or without Symbiodiniaceae), may be fruitful questions for future work. This study sheds new light on the functional diversity of sponge and coral microbiomes and reveals potential metabolic specialization of microbiomes within different invertebrate hosts.

Methods

Sample collection, sequencing, and assembly. The sponge samples of *Xestospongia muta* (n = 3) were collected one each from three Caribbean locations: Conch Reef in the Florida Keys, Rock Bottom Reef near Little Cayman, Cayman Islands, and North Perry Reef near Lee Stocking Island, Bahamas in July and August 2011 as described in¹⁷. The coral samples of brown and orange morph of *Montastraea cavernosa* (n = 3 each) were collected from North Perry Reef near Lee Stocking Island in the Bahamas in August of 2011 and processed as previously described⁵⁵. All samples were collected from approximately 15 m depth; however, *X. muta* samples were collected in the morning (09:00) while the *M. cavernosa* samples were collected around midday. DNA and RNA analyses were conducted with these samples. At each location, maximum photosynthetically active radiation (PAR; 400–700 nm) irradiance is similar, ~500–600 $\mu\text{mol quanta m}^{-2} \text{s}^{-1}$ at noon at each location approx. 15 m depth (M.P. Lesser, unpublished data). There were, however, statistically significant differences in concentrations of NO_3^- (ANOVA, $F_{3,23} = 3.5$, $p = 0.02$, range 0.05–1.2 μM), with the highest average at Little Cayman (0.8 $\mu\text{M} \pm 0.3$). There were no difference in concentrations of NH_4^+ across locations (ANOVA, $F_{3,3,8} = 1.1$, $p = 0.3$, data from Fiore *et al.*⁵⁹).

For marker gene profiling, DNA was extracted, 16S rRNA genes were amplified with PCR, and amplicons were sequenced with 454 pyrosequencing and analyzed using the same protocol within the QIIME (v1) pipeline¹²⁸ as described previously^{55,60}. Methods for OTU generation did not differ significantly between the sponge and coral; identical primers, PCR setup, and initial processing in QIIME to generate OTUs clustered at 97% identity following removal of singleton reads. However, for analysis in this study the OTU sequences from the previous studies^{55,60} were reclassified using the SILVA¹²⁹ release 132.

For metatranscriptome analysis for both coral and sponge, total RNA was extracted, eukaryotic rRNA was removed by subtractive hybridization with a RiboMinus Eukaryote kit (Invitrogen), and reverse transcribed RNA was sequenced using an Illumina HiSeq. 2000 as described previously^{17,55}. The raw RNA reads from each sample were quality trimmed and then used in two separate analyses; short-read analysis of putative mRNA reads and metatranscriptome assembly, forming contiguous sequences (contigs) from the putative mRNA reads. First, in the short-read analysis, the reads were then mapped to SILVA database v.111 and the human genome to remove rRNA and human contamination respectively, using the mapx algorithm by Real Time Genomics (RTG, www.realtimegenomics.com). The remaining unmapped reads, enriched for mRNA, were mapped using the mapx algorithm to approximately ~5000 prokaryotic genomes in the IMG database (available as of February 2013) (<https://img.jgi.doe.gov/>). The reads that mapped to IMG were considered putative prokaryotic mRNA reads and were analyzed for functional annotation with the HUMAnN pipeline⁶⁶ (v.1) using Kyoto Encyclopedia of Genes and Genomes (KEGG⁶⁷). HUMAnN was designed to use metagenomic data to produce a normalized estimate of coverage (presence/absence) and abundance for KEGG metabolic pathways. The pathway coverage, where a pathway consists of two or more genes in that pathway⁶⁶ and abundance (relative abundance per sample) were calculated for all samples. The combined pathway coverage and abundance files were analyzed with STAMP⁶⁸ as described in the main text. Multiple comparisons between the three sample types were calculated using analysis of variance (ANOVA) with Benjamin-Hochberg FDR correction for p -values⁶⁹, and an effect size of 0.8. Pairwise

comparisons between corals and sponges were performed using Welch's *t*-test with Benjamin-Hochberg FDR correction for *p*-values and a relative effect size (i.e., the magnitude of difference between groups⁶⁸) in the ratio proportions of the two groups of 2. In those pairwise comparisons of pathway abundance between sponge and corals, a minimum effect size of 0.8 in the difference between proportions was required, to reduce the number of low abundance pathways that were significantly different but unlikely to be biologically meaningful. Heatmaps were created in STAMP based on significant differences from the multiple comparison analysis. Scatter plots and extended error plots were created in STAMP using mean proportions of abundance or coverage data.

Second, we performed metatranscriptome assembly using quality trimmed RNA reads that did not map to SILVA or to host genomes^{17,55} to produce putative mRNA transcripts using Trinity¹³⁰ as previously described^{17,55}. The same assemblies were used for analysis in the current study, but only the Trinity assembly was used for the sponge metatranscriptome¹⁷ to be consistent with assembly methods for the corals⁵⁵. Sponge RNA reads were quality filtered based on average quality score of 30, a minimum length of 50 nt, removal of adapter sequence and an initial "N" at the start of each reads, and unpaired reads were removed. Briefly, the sponge metatranscriptome was assembled with Trinity and sponge host contiguous sequences (contigs) were distinguished from microbial contigs based on MEGAN¹³¹ analysis as previously described¹⁹. Coral metatranscriptome contigs were assembled with Trinity and BinPacker (<https://goo.gl/Q8pWUu>), then separated into coral host, *Symbiodinium*, and microbial community bins by BLASTX comparison to a custom database comprising RefSeq protein data sets from plants, Bacteria, Archaea, Fungi, Protozoa, and Invertebrates, and a proteome from *Symbiodinium*²¹. The main difference between the sponge and coral assemblies is that a more stringent quality score threshold (Phred <2) was used for corals than for sponges (<30). Here we compare these microbial metatranscriptomes in a transcript presence/absence context only as a means to supplement the short-read analysis. Read and assembly data are available as previously described^{17,55,60} (iMicrobe CAM_P_0000957 (454 pyrosequencing data) and CAM_P_0001214 (metatranscriptome data) sponge; European Nucleotide Archive ID PRJEB18062 (454 pyrosequencing) and DRYAD <https://doi.org/10.5061/dryad.v2g01> (metatranscriptome) coral).

Comparison of total and active microbial communities. The 'total' microbial community was characterized using previously published data of pyrosequencing of 16S rRNA amplicons as described above and in previous work^{55,60}, except that sponge samples were subsampled to a depth of 2200 reads per sample for this study to enable direct comparison with coral samples. The taxonomy of the metabolically 'active' microbial community (i.e., those producing RNA) was characterized by mapping putative mRNA reads to reference prokaryotic genomes in the IMG database, as described above. The taxonomic identity the top hit was captured by the mapx algorithm (see Supplementary Information S2).

Metagenome prediction based on 16S rRNA gene profiling and comparison to metatranscriptome assembly. To complement the metabolic 'snapshot' of the two holobionts generated by the metatranscriptomes and to test the robustness of 16S rRNA-based community function predictions, we compared the metatranscriptome-derived KEGG orthology (KO) to those predicted by 16S rRNA gene profiling. For metagenome prediction, we used the quality trimmed 16S rRNA reads described above with two published programs: PICRUSt v.1.1.3¹³² and Tax4Fun v.0.3.1¹³³. PICRUSt predictions were performed using the precalculated files for the Greengenes v13.5 OTU taxonomy. First, the 16S rRNA OTU table was normalized using the *normalize_by_copy_number.py* script. Secondly, metagenome functional predictions and weighted nearest sequenced taxon index (NSTI) scores for each sample were created using the *predict_metagenomes.py* script. Tax4Fun predictions were performed using the SILVA database (v123) database for QIIME provided by the developer team (<http://tax4fun.gobics.de/>). The fraction of taxonomic units unexplained (FTU) scores by measuring the fraction of sequences assigned to taxonomic units that cannot be mapped to KEGG organisms using the Tax4Fun association matrix. The NSTI and FTU scores serve as a proxy for quality of the respective functional prediction, with a lower score indicating high similarity or correlation between the query 16S rRNA gene sequences and the reference genomes^{132,134}. Metagenomic functional profiles were calculated using the standard parameters (Tax4Fun parameters: refProfile = "UProC", shortReadMode = FALSE, normCopyNo = TRUE).

The resulting KO abundance tables from each prediction were processed with HUMAnN (v.1) to produce pathway coverage estimates for each sponge and coral sample based on KO as described above for the metatranscriptome short-read analysis. Because differences in functional gene expression may not be captured by 16S rRNA gene data, we consider HUMAnN-derived pathway coverage to be a more comparable value than pathway abundance between the metagenome prediction and metatranscriptome data. However, we present both pathway coverage and abundance comparisons, and focus the comparative analysis using pathway coverage.

The predicted KOs were compared with those generated by the metatranscriptome read mapping as described below (under *Functional exploration of metatranscriptomes*). Pearson correlations between the pathway coverage of KOs from the predictions and pathway coverage from the metatranscriptome were performed in R v3.4.0 (R Core Team, 2017), while further community-level comparisons were performed with STAMP v2.1.3⁶⁸.

Functional exploration of metatranscriptomes. Functions and metabolic pathways of interest were identified in metatranscriptomes using both the short-read analysis to provide an overview and assembly method to provide more in-depth analysis of specific metabolic pathways. For the functional overview, we used STAMP to identify all pathways that were differentially present, or differentially expressed, between corals and sponges or between the color morphs of the coral. This analysis was based on the short-read analysis processed with the HUMAnN pipeline (v.1) as described above. The HUMAnN-derived pathway coverage and abundance from each sample were concatenated to form separate 'OTU-type' tables of coverage and abundance for analysis with STAMP. In STAMP, principal components analysis (PCA) was performed and multiple comparisons between the

three sample types were calculated using analysis of variance (ANOVA) with an effect size threshold of 0.8 and Benjamin-Hochberg FDR correction for *p*-values (see Supplementary Information S1).

For the assembly-based investigation of certain metabolic pathways, we selected key elemental cycles and processes on coral reefs based on a review of the literature, including photosynthesis and carbon fixation, the nitrogen cycle, the sulfur cycle, and degradation of xenobiotics, and searched for these metabolic pathways in the metatranscriptome annotations as described below. In this analysis, we used the assembled contiguous sequences (contigs) derived from Trinity algorithms^{17,55} and performed a reanalysis in order to uniformly compare the coral and sponge microbial communities. The RNA pools of *M. cavernosa* and *X. muta* were extracted at the same time, sequenced on the same Illumina HiSeq lane, and were assembled using Trinity, although settings were optimized for each dataset. Thus, while there are caveats such as differences in assembly settings and differences in sampling time between the two assemblies, the comparisons here which are limited to presence/absence of transcripts in metabolic pathways of interest, should be robust enough for foundational comparisons. Assembled transcripts from coral and sponge were translated into protein sequences with prodigal (v2.6.3) using the -meta flag, and KO numbers were assigned to proteins (genus_prokaryotes + family_eukaryotes) with GhostKOALA¹³³. Proteins present from each pathway of interest were collected and the resulting pathway files were viewed in Pathview¹³⁵ to compare presence/absence of KOs for each microbiome community. The use of assembled contigs here allowed us to capture visualize the presence and taxonomic identity of transcripts that correspond to specific genes within metabolic pathways of interest. Such fine-scale information was not possible with the short-read analysis processed with the HUMAnN pipeline.

Received: 4 October 2018; Accepted: 27 January 2020;

Published online: 11 February 2020

References

1. Oliver, K. M., Moran, N. A. & Hunter, M. S. Variation in resistance to parasitism in aphids is due to symbionts not host genotype. *Proc. Natl. Acad. Sci. USA* **102**, 12795–800 (2005).
2. Wright, D. P., Scholes, J. D. & Read, D. J. Effects of VA mycorrhizal colonization on photosynthesis and biomass production of *Trifolium repens* L. *Plant, Cell Environ.* **21**, 209–216 (1998).
3. Moran, N. A., Tran, P. & Gerardo, N. M. Symbiosis and insect diversification: an ancient symbiont of sap-feeding insects from the bacterial phylum Bacteroidetes. *Appl. Environ. Microbiol.* **71**, 8802–10 (2005).
4. Muscatine, L. Glycerol excretion by symbiotic algae from corals and *Tridacna* and its control by the host. *Science* (80-). **156**, 516–519 (1967).
5. Muscatine, L. & Porter, J. W. Reef Corals: Mutualistic Symbioses Adapted to Nutrient-Poor Environments. *Bioscience* **27**, 454–460 (1977).
6. Diaz, M. C. & Rützler, K. Sponges: An Essential Component Of Caribbean Coral Reefs. *Bull. Mar. Sci.* **69**, 535–546 (2001).
7. Ainsworth, T. D., Thurber, R. V. & Gates, R. D. The future of coral reefs: a microbial perspective. *Trends Ecol. Evol.* **25**, 233–240 (2010).
8. Fiore, C. L., Jarett, J. K., Olson, N. D. & Lesser, M. P. Nitrogen fixation and nitrogen transformations in marine symbioses. *Trends Microbiol.* **18**, 455–463 (2010).
9. Hernandez-Agreda, A., Gates, R. D. & Ainsworth, T. D. Defining the Core Microbiome in Corals' Microbial Soup. *Trends Microbiol.* **25**, 125–140 (2017).
10. Piel, J. Metabolites from symbiotic bacteria. *Nat. Prod. Rep.* **26**, 338–362 (2009).
11. Kwan, J. C. *et al.* Genome streamlining and chemical defense in a coral reef symbiosis. *Proc. Natl. Acad. Sci. USA* **109**, 20655–60 (2012).
12. Hoffmann, F. *et al.* Complex nitrogen cycling in the sponge *Geodia barretti*. *Environ. Microbiol.* **11**, 2228–2243 (2009).
13. Li, Z. *et al.* Metagenomic Analysis of Genes Encoding Nutrient Cycling Pathways in the Microbiota of Deep-Sea and Shallow-Water Sponges. *Mar. Biotechnol.* **18**, 659–671 (2016).
14. Lesser, M., Mazel, C., Gorbunov, M. & Falkowski, P. Discovery of symbiotic nitrogen-fixing cyanobacteria in corals. *Science* (80-). **305**, 997–1000 (2004).
15. Mohamed, N. M., Colman, A. S., Tal, Y. & Hill, R. T. Diversity and expression of nitrogen fixation genes in bacterial symbionts of marine sponges. *Environ. Microbiol.* **10**, 2910–2921 (2008).
16. Freeman, C. J. & Thacker, R. W. Complex interactions between marine sponges and their symbiotic microbial communities. *Limnol. Oceanogr.* **56**, 1577–1586 (2011).
17. Fiore, C. L., Labrie, M., Jarett, J. K. & Lesser, M. P. Transcriptional activity of the giant barrel sponge, *Xestospongia muta* Holobiont: molecular evidence for metabolic interchange. *Front. Microbiol.* **6** (2015).
18. Bourne, D. G., Morrow, K. M. & Webster, N. S. Insights into the Coral Microbiome: Underpinning the Health and Resilience of Reef Ecosystems. *Annu. Rev. Microbiol.* **70**, 317–340 (2016).
19. Thomas, T. *et al.* Diversity, structure and convergent evolution of the global sponge microbiome. *Nat. Commun.* **7** (2016).
20. Moitinho-Silva, L. *et al.* The sponge microbiome project. *Gigascience* **6**, 1–7 (2017).
21. Blackall, L. L., Wilson, B. & van Oppen, M. J. H. Coral-the world's most diverse symbiotic ecosystem. *Mol. Ecol.* **24**, 5330–5347 (2015).
22. Cleary, D. F. R. *et al.* The sponge microbiome within the greater coral reef microbial metacommunity. *Nat. Commun.* **10**, 1644 (2019).
23. Morrow, K. M., Muller, E. & Lesser, M. P. How Does the Coral Microbiome Cause, Respond to, or Modulate the Bleaching Process? in 153–188, https://doi.org/10.1007/978-3-319-75393-5_7 (Springer, Cham, 2018).
24. Haridim, C. C. P. & Costa, R. Temporal dynamics of prokaryotic communities in the marine sponge *Sarcotragus spinosulus*. *Mol. Ecol.* **23**, 3097–3112 (2014).
25. Gantt, S. E., López-Legentil, S. & Erwin, P. M. Stable microbial communities in the sponge *Crambe crambe* from inside and outside a polluted Mediterranean harbor. *FEMS Microbiol. Lett.* **364** (2017).
26. Dunphy, C. M., Gouhier, T. C., Chu, N. D. & Vollmer, S. V. Structure and stability of the coral microbiome in space and time. *Sci. Rep.* **9**, 6785 (2019).
27. Sweet, M. J., Brown, B. E., Dunne, R. P., Singleton, I. & Bulling, M. Evidence for rapid, tide-related shifts in the microbiome of the coral *Coelastrea aspera*. *Coral Reefs* **36**, 815–828 (2017).
28. Easson, C. G. & Thacker, R. W. Phylogenetic signal in the community structure of host-specific microbiomes of tropical marine sponges. *Front. Microbiol.* **5**, 532 (2014).
29. Rohwer, F., Seguritan, V., Azam, F. & Knowlton, N. Diversity and distribution of coral-associated bacteria. *Mar. Ecol. Prog. Ser.* **243**, 1–10 (2002).

30. Littman, R. A., Willis, B. L., Pfeffer, C. & Bourne, D. G. Diversities of coral-associated bacteria differ with location, but not species, for three acroporid corals on the Great Barrier Reef. *FEMS Microbiol. Ecol.* **68**, 152–163 (2009).
31. Roder, C., Bayer, T., Aranda, M., Kruse, M. & Voolstra, C. R. Microbiome structure of the fungid coral *Ctenactis echinata* aligns with environmental differences. *Mol. Ecol.* **24**, 3501–3511 (2015).
32. Taylor, M. W., Radax, R., Steger, D. & Wagner, M. Sponge-associated microorganisms: evolution, ecology, and biotechnological potential. *Microbiol. Mol. Biol. Rev.* **71**, 295–347 (2007).
33. Pita, L., Rix, L., Slaby, B. M., Franke, A. & Hentschel, U. The sponge holobiont in a changing ocean: from microbes to ecosystems. *Microbiome* **6**, 46 (2018).
34. Weisz, J. B., Massaro, A. J., Ramsby, B. D. & Hill, M. S. Zooxanthellar symbionts shape host sponge trophic status through translocation of carbon. *Biol. Bull.* **219**, 189–197 (2010).
35. Freeman, C., Thacker, R., Baker, D. & Fogel, M. Quality or quantity: is nutrient transfer driven more by symbiont identity and productivity than by symbiont abundance? *ISME J.* **7**, 116–1125 (2013).
36. Moitinho-Silva, L. *et al.* Specificity and transcriptional activity of microbiota associated with low and high microbial abundance sponges from the Red Sea. *Mol. Ecol.* **23**, 1348–1363 (2014).
37. Moitinho-Silva, L. *et al.* Integrated metabolism in sponge–microbe symbiosis revealed by genome-centered metatranscriptomics. *ISME J.* **11**, 1651–1666 (2017).
38. Daniels, C. A. *et al.* Metatranscriptome analysis of the reef-building coral *Orbicella faveolata* indicates holobiont response to coral disease. *Front. Mar. Sci.* **2**, 62 (2015).
39. Yang, S.-H. *et al.* Metagenomic, phylogenetic, and functional characterization of predominant endolithic green sulfur bacteria in the coral *Isopora palifera*. *Microbiome* **7**, 3 (2019).
40. Jensen, S. *et al.* The Relative Abundance and Transcriptional Activity of Marine Sponge-Associated Microorganisms Emphasizing Groups Involved in Sulfur Cycle. *Microb. Ecol.* **73**, 668–676 (2017).
41. Raina, J.-B. *et al.* Isolation of an antimicrobial compound produced by bacteria associated with reef-building corals. *PeerJ* **4**, e2275 (2016).
42. Thomas, S. *et al.* Evidence for phosphonate usage in the coral holobiont. *ISME J.* **4**, 459–461 (2010).
43. Zhang, F. *et al.* Phosphorus sequestration in the form of polyphosphate by microbial symbionts in marine sponges. *Proc. Natl. Acad. Sci. USA* **112**, 4381–6 (2015).
44. De Goeij, J. M., Van Den Berg, H., Van Oostveen, M. M., Epping, E. H. G. & Van Duyl, F. C. Major bulk dissolved organic carbon (DOC) removal by encrusting coral reef cavity sponges. *Mar. Ecol. Prog. Ser.* **357**, 139–151 (2008).
45. Lai, S. *et al.* First experimental evidence of corals feeding on seagrass matter. *Coral Reefs* **32**, 1061–1064 (2013).
46. Fiore, C. L., Freeman, C. J. & Kujawinski, E. B. Sponge exhalant seawater contains a unique chemical profile of dissolved organic matter. *PeerJ* **5**, e2870 (2017).
47. Rix, L. *et al.* Differential recycling of coral and algal dissolved organic matter via the sponge loop. *Funct. Ecol.* **31**, 778–789 (2017).
48. Achlatis, M. *et al.* Sponge bioerosion on changing reefs: ocean warming poses physiological constraints to the success of a photosymbiotic excavating sponge. *Sci. Rep.* **7**, 10705 (2017).
49. Foster, K. R., Schluter, J., Coyte, K. Z. & Rakoff-Nahoum, S. The evolution of the host microbiome as an ecosystem on a leash. *Nature* **548**, 43–51 (2017).
50. Lavy, A., Keren, R., Yahel, G. & Ilan, M. Intermittent hypoxia and prolonged suboxia measured *in situ* in a marine sponge. *Front. Mar. Sci.* **3**, 263 (2016).
51. Sweet, M. J., Croquer, A. & Bythell, J. C. Bacterial assemblages differ between compartments within the coral holobiont. *Coral Reefs* **30**, 39–52 (2011).
52. Köhl, M., Cohen, Y., Dalsgaard, T., Jørgensen, B. B. & Revsbech, N. P. Microenvironment and photosynthesis of zooxanthellae in scleractinian corals studied with microensors for O₂, pH and light. *Marine Ecology Progress Series* **117** (1995).
53. Fan, L. *et al.* Functional equivalence and evolutionary convergence in complex communities of microbial sponge symbionts. *Proc. Natl. Acad. Sci. U. S. A.* E1878–E1887, <https://doi.org/10.1073/pnas.97.18.10008> (2012).
54. Dinsdale, E. A. *et al.* Functional metagenomic profiling of nine biomes. *Nature* **452**, 629–632 (2008).
55. Jarett, J. K., MacManes, M. D., Morrow, K. M., Pankey, M. S. & Lesser, M. P. Comparative genomics of color morphs in the coral *Montastraea cavernosa*. *Sci. Rep.* **7**, 16039 (2017).
56. Thompson, L. R. *et al.* The Earth Microbiome Project Consortium. A communal catalogue reveals Earth's multiscale microbial diversity. *Nature* **551**, 457–463 (2017).
57. Southwell, M. W., Weisz, J. B., Martens, C. S. & Lindquist, N. *In situ* fluxes of dissolved inorganic nitrogen from the sponge community on Conch Reef, Key Largo, Florida. *Limnol. Oceanogr.* **53**, 986–996 (2008).
58. McMurray, S. E., Blum, J. E. & Pawlik, J. R. Redwood of the reef: growth and age of the giant barrel sponge *Xestospongia muta* in the Florida Keys. *Mar. Biol.* **155**, 159–171 (2008).
59. Fiore, C. L., Baker, D. M. & Lesser, M. P. Nitrogen Biogeochemistry in the Caribbean Sponge, *Xestospongia muta*: A Source or Sink of Dissolved Inorganic Nitrogen? *PLoS One* **8**, e72961 (2013).
60. Fiore, C. L., Jarett, J. K. & Lesser, M. P. Symbiotic prokaryotic communities from different populations of the giant barrel sponge, *Xestospongia muta*. *Microbiologyopen* **2**, 938–952 (2013).
61. Beckers, B., De Beeck, O., Weyens, N., Boerjan, W. & Vangronsveld, J. Structural variability and niche differentiation in the rhizosphere and endosphere bacterial microbiome of field-grown poplar trees. *Microbiome* **5**, 25 (2017).
62. Tannock, G. W. *et al.* Resource partitioning in relation to cohabitation of *Lactobacillus* species in the mouse forestomach. *ISME J.* **6**, 927–938 (2012).
63. Consortium, T. H. M. P. *et al.* Structure, function and diversity of the healthy human microbiome. *Nature* **486**, 207–214 (2012).
64. Taxis, T. M. *et al.* The players may change but the game remains: network analyses of ruminal microbiomes suggest taxonomic differences mask functional similarity. *Nucleic Acids Res.* **43**, 9600–9612 (2015).
65. Phillips, C. D. *et al.* Microbiome Structural and Functional Interactions across Host Dietary Niche Space. *Integr. Comp. Biol.* **57**, 743–755 (2017).
66. Abubucker, S. *et al.* Metabolic Reconstruction for Metagenomic Data and Its Application to the Human Microbiome. *PLoS Comput. Biol.* **8**, e1002358 (2012).
67. Kanehisa, M. & Goto, S. KEGG: Kyoto encyclopedia of genes and genomes. *Nucleic Acids Res.* **28**, 27–30 (2000).
68. Parks, D. H., Tyson, G. W., Hugenholtz, P. & Beiko, R. G. STAMP: statistical analysis of taxonomic and functional profiles. *Bioinformatics* **30**, 3123–3124 (2014).
69. Benjamini, Y. & Hochberg, Y. Controlling the false discovery rate: a practical and powerful approach to multiple testing. *Journal of the Royal Statistical Society. Series B (Methodological)* **57**, 289–300 (1995).
70. Botté, E. S. *et al.* Changes in the metabolic potential of the sponge microbiome under ocean acidification. *Nat. Comm.* (2019).
71. Tilstra, A. *et al.* Denitrification aligns with N₂ fixation in Red Sea corals. *Sci. Reports.* **9**, 19460 (2019).
72. Siboni, N., Ben-Dov, E., Sivan, A. & Kushmaro, A. Global distribution and diversity of coral-associated *Archaea* and their possible role in the coral holobiont nitrogen cycle. *Environ. Microbiol.* **10**, 2979–2990 (2008).
73. Wafar, M., Wafar, S. & David, J. J. Nitrification in reef corals. *Limnol. Oceanogr.* **35**, 725–730 (1990).
74. Rädicker, N., Pogoreutz, C., Voolstra, C. R., Wiedenmann, J. & Wild, C. Nitrogen cycling in corals: the key to understanding holobiont functioning? *Trends Microbiol.* **23**, 490–497 (2015).

75. Schulz, A. A., Collett, H. J. & Reid, S. J. Nitrogen and carbon regulation of glutamine synthetase and glutamate synthase in *Corynebacterium glutamicum* ATCC 13032. *FEMS Microbiol. Lett.* **205**, 361–367 (2001).
76. Tsukada, S. *et al.* Comparative genome-wide transcriptional profiling of *Azorhizobium caulinodans* ORS571 grown under free-living and symbiotic conditions. *Appl. Environ. Microbiol.* **75**, 5037–46 (2009).
77. Tian, R.-M. *et al.* Genome analysis reveals versatile heterotrophic capacity of a potentially symbiotic sulfur-oxidizing bacterium in sponge. *Environ. Microbiol.* **16**, 3548–3561 (2014).
78. Tian, R. M. *et al.* Genome reduction and microbe-host interactions drive adaptation of a sulfure-oxidizing bacterium associated with a cold seep sponge. *mSystems*. **21**, 2 (2017).
79. Cai, L. *et al.* Metagenomic analysis reveals a green sulfur bacterium as a potential coral symbiont. *Sci. Rep.* **7**, 9320 (2017).
80. Kleiner, M., Petersen, J. M. & Dubilier, N. Convergent and divergent evolution of metabolism in sulfur-oxidizing symbionts and the role of horizontal gene transfer. *Curr. Opin. Microbiol.* **15**, 621–631 (2012).
81. Platen, H. & Schink, B. Anaerobic Degradation of Acetone and Higher Ketones via Carboxylation by Newly Isolated Denitrifying Bacteria. *Microbiology* **135**, 883–891 (1989).
82. Wackett, L. P., Brusseau, G. A., Householder, S. R. & Hanson, R. S. Survey of microbial oxygenases: trichloroethylene degradation by propane-oxidizing bacteria. *Appl. Environ. Microbiol.* **55**, 2960–4 (1989).
83. Ravi, B. N. & Faulkner, D. J. Cembranoid diterpenes from a South Pacific soft coral. *J. Org. Chem.* **43**, 2127–2131 (1978).
84. Bowling, J. J., Mohammed, R., Diers, J. A. & Hamann, M. T. Abundant ketone isolated from oily *Plakortis* sponge demonstrates antifouling properties. *Chemoecology* **20**, 207–213 (2010).
85. Jarett, J. K., Gochfeld, D. J. & Lesser, M. P. Aposematic coloration does not deter corallivory by fish on the coral *Montastraea cavernosa*. *Coral Reefs* **35**, 883–887 (2016).
86. Kittredge, J. S. & Roberts, E. A carbon-phosphorus bond in nature. *Science* **164**, 37–42 (1969).
87. Hilderbrand, R. L. *The Role of phosphonates in living systems*. (CRC Press, 1983).
88. Ferrier-Pagès, C., Godinot, C., D'Angelo, C., Wiedenmann, J. & Grover, R. Phosphorus metabolism of reef organisms with algal symbionts. *Ecol. Monogr.* **86**, 262–277 (2016).
89. Godinot, C., Gaysinski, M., Thomas, O. P., Ferrier-Pagès, C. & Grover, R. On the use of ³¹P NMR for the quantification of hydrosoluble phosphorus-containing compounds in coral host tissues and cultured zooxanthellae. *Sci. Rep.* **6**, 21760 (2016).
90. Clark, L. L. Marine organic phosphorus cycling: novel insights from nuclear magnetic resonance. *Am. J. Sci.* **299**, 724–737 (1999).
91. Ilikchyan, I. N., McKay, R. M. L., Zehr, J. P., Dyhrman, S. T. & Bullerjahn, G. S. Detection and expression of the phosphonate transporter gene *phnD* in marine and 96. Pilson, M. E. Q. & Betzer, S. B. Phosphorus flux across a coral reef. *Ecology* **54**, 581–588 (1973).
92. Pilson, M. E. Q. & Betzer, S. B. Phosphorus flux across a coral reef. *Ecology* **54**, 581–588 (1973).
93. Larned, S. T. Nitrogen- versus phosphorus-limited growth and sources of nutrients for coral reef macroalgae. *Mar. Biol.* **132**, 409–421 (1998).
94. Cleary, D. F. R., Polonia, A. R. M. & de Voogd, N. J. Prokaryotic composition and predicted metagenomic content of two *Cinachyrella* morphospecies and water from West Papuan Marine Lakes. *FEMS Microbiol. Lett.* **94**, fix175 (2018).
95. Boyd, P. W. & Ellwood, M. J. The biogeochemical cycle of iron in the ocean. *Nat. Geosci.* **3**, 675–682 (2010).
96. Sun, Y. & Sun, M. Determination of 42 Trace Elements in Seawater by Inductively Coupled Plasma Mass Spectrometry After APDC Chelate Co-precipitation Combined With Iron. *Anal. Lett.* **40**, 2391–2404 (2007).
97. Ceapă, C. D. *et al.* Genome mining of *Streptomyces scabrisporus* NF3 reveals symbiotic features including genes related to plant interactions. *PLoS One* **13**, e0192618 (2018).
98. Vacheron, J. *et al.* Plant growth-promoting rhizobacteria and root system functioning. *Front. Plant Sci.* **4** (2013).
99. Flores-Félix, J. D. *et al.* Plants probiotics as a tool to produce highly functional fruits: the case of *Phyllobacterium* and vitamin C in strawberries. *PLoS One* **10**, e0122281 (2015).
100. Fischbach, M. A., Lin, H., Liu, D. R. & Walsh, C. T. How pathogenic bacteria evade mammalian sabotage in the battle for iron. *Nat. Chem Biol.* **2**, 132–138 (2006).
101. Cárdenas, A. *et al.* Excess labile carbon promotes the expression of virulence factors in coral reef bacterioplankton. *ISME J.* **12**, 59–76 (2018).
102. Özkaya, F. C., Bedir, E. & Hameş, E. E. A new siderophore from sponge associated *Pseudomonas Fluorescens* 4.9.3. *Rec. Nat. Prod.* **9**, 509–517 (2015).
103. Milanese, M. *et al.* The marine sponge *Chondrilla nucula* Schmidt, 1862 as an elective candidate for bioremediation in integrated aquaculture. *Biomol. Eng.* **20**, 363–368 (2003).
104. Steinert, G. *et al.* Prokaryotic diversity and community patterns in Antarctic continental shelf sponges. *Front. Mar. Sci.* **6**, 297 (2019).
105. Brinkmann, C. M., Marker, A. & Kurtböke, D. I. An overview on marine sponge-symbiotic bacteria as unexhausted sources for natural product discovery. *Diversity*. **9**, 40 (2017).
106. Patil, A. D. *et al.* Brominated polyacetylenic acids from the marine sponge *Xestospongia muta*: inhibitors of HIV protease. *J. Nat. Prod.* **55**, 1170–1177 (1992).
107. Villegas-Plazas, M. *et al.* Variations in microbial diversity and metabolite profiles of the tropical marine sponge *Xestospongia muta* with season and depth. *Microb. Ecol.* **78**, 243–256 (2019).
108. Claus, G., Madri, P. & Kunen, S. Removal of microbial pollutants from waste effluents by the redbeard sponge. *Nature* **216**, 712–714 (1967).
109. Brown, D. W., Adams, T. H. & Keller, N. P. Aspergillus has distinct fatty acid synthases for primary and secondary metabolism. *Proc. Natl. Acad. Sci.* **93**, 14873–14877 (1996).
110. Giordano, D. *et al.* Chapter four - marine microbial secondary metabolites: pathways, evolution and physiological roles. *Advanc. Microb. Phys.* **66**, 357–428 (2015).
111. Blackall, L. L., Wilson, B. & Van Oppen, M. J. H. Coral - the world's most diverse symbiotic ecosystem. *Molec. Ecol.* **24**, 5330–5347 (2015).
112. Imhoff, J. F., Rahn, T., Künzel, S. & Neulinger, S. C. Photosynthesis Is Widely Distributed among Proteobacteria as Demonstrated by the Phylogeny of PufLM Reaction Center Proteins. *Front. Microbiol.* **8**, 2679 (2018).
113. Naumann, M., Richter, C., el-Zibdah, M. & Wild, C. Coral mucus as an efficient trap for picoplanktonic cyanobacteria: implications for pelagic-benthic coupling in the reef ecosystem. *Mar. Ecol. Prog. Ser.* **385**, 65–76 (2009).
114. McNally, S. P., Parsons, R. J., Santoro, A. E. & Apprill, A. Multifaceted impacts of the stony coral *Porites astreoides* on picoplankton abundance and community composition. *Limnol. Oceanogr.* **62**, 217–234 (2017).
115. Ducklow, H. W. & Mitchell, R. Bacterial populations and adaptations in the mucus layers on living corals I. *Limnol. Oceanogr.* **24**, 715–725 (1979).
116. Kwong, W. K., Del Campo, J., Mathur, V., Vermeij, M. J. A. & Keeling, P. J. A widespread coral-infecting apicomplexan with chlorophyll biosynthesis genes. *Nature* **568**, 103–107 (2019).
117. Montalvo, N. F. & Hill, R. T. Sponge-associated bacteria are strictly maintained in two closely related but geographically distant sponge hosts. *Appl. Environ. Microbiol.* **77**, 7207–7216 (2011).
118. Morrow, K. M., Fiore, C. L. & Lesser, M. P. Environmental drivers of microbial community shifts in the giant barrel sponge, *Xestospongia muta*, over a shallow to mesophotic depth gradient. *Environ. Microbiol.* **18**, 2025–38 (2016).

119. Ritchie, K. B. & Smith, G. W. Microbial Communities of Coral Surface Mucopolysaccharide Layers. in *Coral Health and Disease* 259–264, https://doi.org/10.1007/978-3-662-06414-6_13 (Springer Berlin Heidelberg, 2004).
120. McCutchen, J. P., McDonald, B. R. & Moran, N. A. Convergent evolution of metabolic roles in bacterial co-symbionts of insects. *Proc. Natl. Acad. Sci. USA* **106**, 14288–14293 (2011).
121. Ribes, M. *et al.* Functional convergence of microbes associated with temperate marine sponges. *Environ. Microbiol.* **14**, 1224–1239 (2012).
122. Webster, N. S. & Thomas, T. The sponge hologenome. *mBio*. **7**, e00135–16 (2016).
123. Talbot, J. M. *et al.* Endemism and functional convergence across the North American soil mycobiome. *Proc. Natl. Acad. Sci. USA* **111**, 6341–6346 (2014).
124. Burke, C., Steinberg, P., Rusch, D., Kjelleberg, S. & Thomas, T. Bacterial community assembly based on functional genes rather than species. **108**, 14288–14293 (2005).
125. Rennison, D. J., Rudman, S. M. & Schluter, D. Parallel changes in gut microbiome composition and function during colonization, local adaptation and ecological speciation. *Proc. R. Soc. B.* **286**, 20191911 (2019).
126. Rao, N. N., Gómez-García, M. R. & Kornberg, A. Inorganic polyphosphate essential for growth and survival. *Annu. Rev. Biochem.* **78**, 605–647 (2009).
127. Coleman, A. S. Sponge symbionts and the marine P cycle. *Proc. Natl. Acad. Sci. USA* **112**, 4191–4192 (2015).
128. Caporaso, J. G. *et al.* QIIME allos analysis of high-throughput community sequencing data. *Nature Meth.* **7**, 335–336 (2010).
129. Quast, C. *et al.* The SILVA ribosomal RNA gene database project: improved data processing and web-based tools. *Nucleic Acids Res.* **41**, D590–D596 (2013).
130. Grabherr, M. G. *et al.* Full-length transcriptome assembly from RNA-Seq data without a reference genome. *Nat. Biotechnol.* **29**, 644–652 (2011).
131. Huson, D. H., Auch, A. F., Qi, J. & Schuster, S. C. MEGAN analysis of metagenomic data. *Gen. Res.* **17**, 377–386 (2007).
132. Aßhauer, K. P., Wemheuer, B., Daniel, R. & Meinicke, P. Tax4Fun: predicting functional profiles from metagenomic 16S rRNA data. *Bioinformatics* **31**, 2882–2884 (2015).
133. Kanehisa, M., Sato, Y. & Morishima, K. BlastKOALA and GhostKOALA: KEGG tools for functional characterization of genome and metagenome sequences. *J. Molec. Biol.* **428**, 726–731 (2016).
134. Langille, M. G. I. *et al.* Predictive functional profiling of microbial communities using 16S rRNA marker gene sequences. *Nat. Biotechnol.* **31**, 814–821 (2013).
135. Luo, W., Pant, G., Bhavnasi, Y. K., Blanchard, S. G. & Brouwer, C. Pathview web: user friendly pathway visualization and data integration. *Nucl acids Res* **45**, W501–508 (2017).

Acknowledgements

We thank M. Slattery, D. Gochfeld, and L. Kintzing for assistance with field collections. All collections were made under permits for the Bahamas (MA/FIS/1, 12, 46, 79) and the United States (CITES Permit 2011/186). We are grateful to two anonymous reviewers for improvements to this manuscript. This research was supported by the National Science Foundation grants OCE 1231468, 1437054, and 1638296 (Dimensions of Biodiversity) to MPL, and JKJ was supported by an NSF Graduate Research Fellowship Program grant (DCE 0913620).

Author contributions

C.L.F., J.K.J. and M.P.L. designed and conducted the collections and experiments. J.K.J. and C.L.F. prepared samples for transcriptomics sequencing. C.L.F., J.K.J. and G.S. performed all data analysis. C.L.F., J.K.J., G.S. and M.P.L. wrote and approved the content of the manuscript.

Competing interests

The authors declare no competing interests.

Additional information

Supplementary information is available for this paper at <https://doi.org/10.1038/s41598-020-59320-9>.

Correspondence and requests for materials should be addressed to C.L.F.

Reprints and permissions information is available at www.nature.com/reprints.

Publisher's note Springer Nature remains neutral with regard to jurisdictional claims in published maps and institutional affiliations.



Open Access This article is licensed under a Creative Commons Attribution 4.0 International License, which permits use, sharing, adaptation, distribution and reproduction in any medium or format, as long as you give appropriate credit to the original author(s) and the source, provide a link to the Creative Commons license, and indicate if changes were made. The images or other third party material in this article are included in the article's Creative Commons license, unless indicated otherwise in a credit line to the material. If material is not included in the article's Creative Commons license and your intended use is not permitted by statutory regulation or exceeds the permitted use, you will need to obtain permission directly from the copyright holder. To view a copy of this license, visit <http://creativecommons.org/licenses/by/4.0/>.

© The Author(s) 2020